American Mineralogist, Volume 84, pages 214–220, 1999

High-resolution synchrotron X-ray powder diffraction and Rietveld structure refinement of two $(Mg_{0.95},Fe_{0.05})SiO_3$ perovskite samples synthesized under different oxygen fugacity conditions

A.P. JEPHCOAT,[1,*] J.A. HRILJAC,[2] C.A. MCCAMMON,[3] H. ST.C. O'NEILL,[3] D.C. RUBIE,[3] AND L.W. FINGER[4]

[1]Department of Earth Sciences, University of Oxford, Parks Road, Oxford, OX1 3PR U.K.
[2]Department of Applied Science, Chemical Sciences Division, Brookhaven National Laboratory, P.O. Box 5000, Building 815, Upton, Long Island, New York 11973–5000, U.S.A.
[3]Bayerisches Geoinstitut, Universität Bayreuth, 95440 Bayreuth, Germany
[4]Center for High-Pressure Research and Geophysical Laboratory, 5251 Broad Branch Road, N.W., Washington, D.C. 20015–1305, U.S.A.

ABSTRACT

This paper presents high-resolution synchrotron X-ray powder diffraction data at 290 K on two Fe-bearing, polycrystalline silicate perovskite samples with approximate compositions $(Mg_{0.95}Fe_{0.05})SiO_3$ synthesized at 25 GPa and 1920 K in a multi-anvil press at different oxygen fugacity conditions. Mössbauer studies have indicated that $Fe^{3+}/\Sigma Fe$ for the samples are 0.09 ± 0.01 and near 0.16 ± 0.03. Rietveld structural refinements confirm that Fe^{2+} and Fe^{3+} dominantly substitute for Mg^{2+} in the 8-fold to 12-fold coordinated A site for both compositions. There appears to be no significant differences in the bond distances for these amounts of Fe^{3+} and no conclusive structural evidence to support indications from Mössbauer experiments that Fe^{3+} may occupy both A and B sites. To explore the effect of valence state further, this study also reports the first diffraction patterns of $(Mg,Fe)SiO_3$ perovskite collected at a wavelength near the Fe absorption edge.

INTRODUCTION

The expected dominance of $(Mg,Fe)SiO_3$ with the perovskite structure in the Earth's lower mantle has prompted extensive studies of its crystal chemistry, thermodynamic properties, and transport properties (see Hemley and Cohen 1992, for review). In ferromagnesian perovskites the site occupancy of Fe in $(Mg,Fe)SiO_3$ as a function of oxidation state has been investigated for several compositions by both Mössbauer and optical techniques (Keppler et al. 1994; Fei et al. 1994; Shen et al. 1994; McCammon 1998) and is a particularly important aspect of the crystal chemistry. Studies on the partitioning of Fe^{3+} between perovskite and magnesiowüstite and electrical conductivity measurements (Wood and Nell 1991; Poirier et al. 1996) have shown that subtle changes in the cation site and valence could be important macroscopically and could determine lower-mantle electrical conductivity. Thermally activated electron delocalization and electron exchange between Fe^{3+} in the octahedral site and Fe^{2+} polyhedra have been suggested as a likely explanation of the wide variation in electrical conductivity observed in ferromagnesian perovskites (Fei et al. 1994). The hyperfine parameters obtained in Mössbauer studies suggest that Fe^{3+} occupies the octahedral site (McCammon et al. 1992; Fei at al. 1994; McCammon 1998). We compare the structural parameters obtained in these studies with the present samples.

Advances in the understanding of perovskite crystal chemistry have been made possible largely through widespread development of multi-anvil techniques at high pressures and temperatures leading to the synthesis of high-quality silicate perovskites of varying (Fe + Mg)/Si stoichiometry and, more recently, oxidation state. Independent advances in high-resolution synchrotron X-ray diffraction (XRD) techniques (Cox 1991, and references therein), make possible detailed structure refinements from powder X-ray data and are suited to analysis of samples from multi-anvil experiments that generally produce polycrystalline, multiphase products. Detailed structural studies have been reported for several ferromagnesian perovskite compositions periodically in the last decade by both powder and single-crystal techniques (Ito and Yamada 1982; Parise et al. 1990; Kudoh et al. 1990) with particular attention to Fe distribution between A and B sites. Structural data for perovskites with the conventional Fe-Mg stoichiometry, characterized by Mössbauer techniques, can serve as a point of reference for studying detailed effects of valence state, charge transfer, defects, and trace-element substitution.

Presented here are the results of high-resolution synchrotron powder XRD study of quenched ferromagnesian perovskites with two slightly different oxidation states

* E-mail: andrew@earth.ox.ac.uk

0003–004X/99/0003–0214$05.00

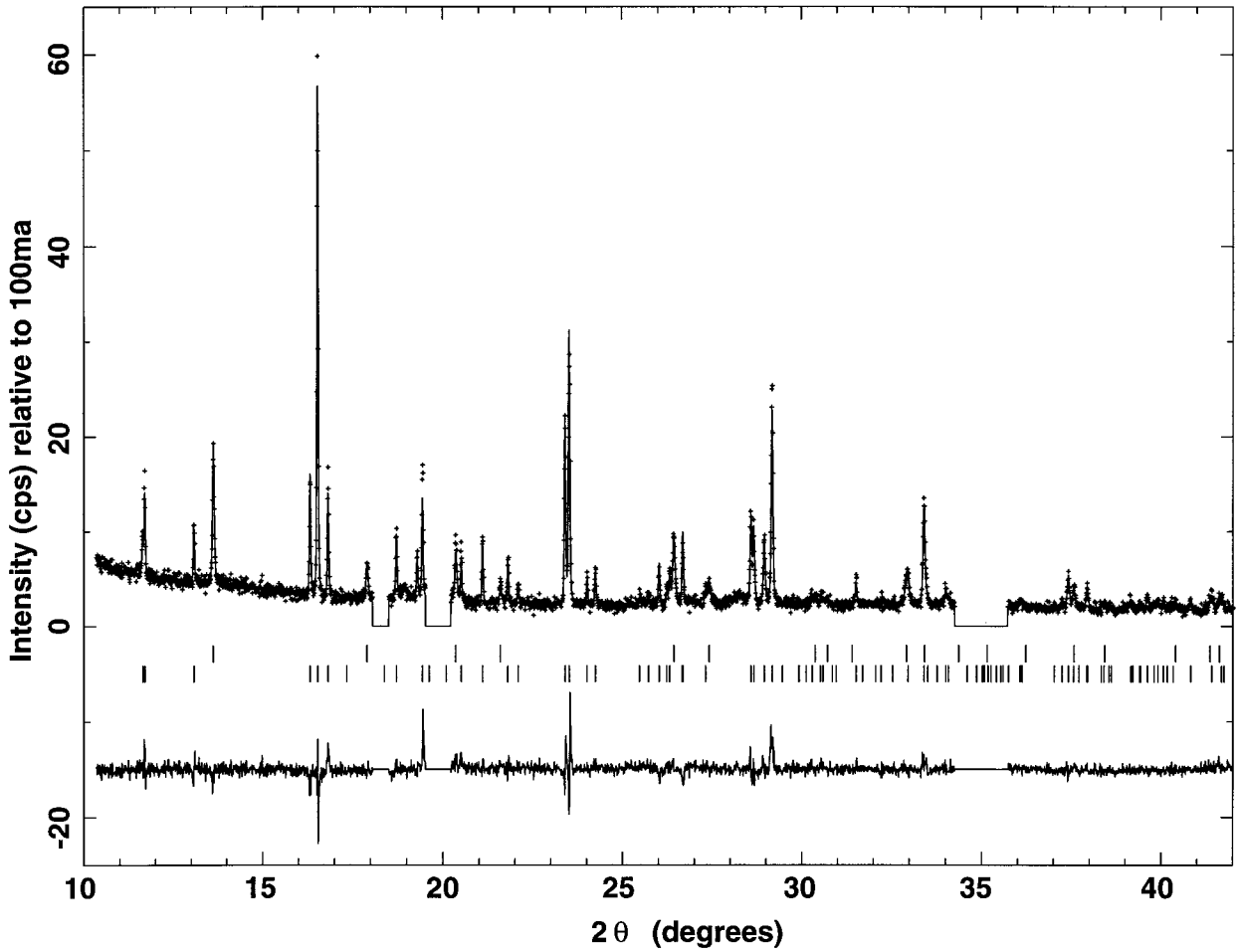

FIGURE 1. Observed (crosses), calculated (solid line) and difference profile (bottom) from the Rietveld analysis of Sample A. The tick marks below the observed pattern indicate allowed peak positions for PV-A (lower) and stishovite (upper). Flat regions shown at zero counts were excluded from the refinement.

synthesized by multi-anvil techniques and extensively characterized by Mössbauer spectroscopy (McCammon et al. 1992; McCammon 1998). Independent assessment of the site occupancy refinement has been attempted through resonant X-ray diffraction near the Fe K-edge to detect differences in the anomalous scattering power from the two possible sites. Such studies offer the potential to examine the Fe positions as a function of valence state (Warner et al. 1992).

EXPERIMENTAL PROCEDURES

Two perovskite compositions, denoted PV-A and PV-B, were synthesized in the multi-anvil apparatus at the Bayerisches Geoinstitut following methods described by McCammon et al. (1992). Sample A, containing PV-A, was formed by transforming clinoenstatite starting material to perovskite at 25 GPa and 1900 K in an Fe capsule with 5 wt% Fe metal and 5 wt% SiO_2 quartz. The perovskite in this sample, therefore, was synthesized under the lowest possible oxygen fugacity conditions at which this composition is stable, and should contain the minimum amount of Fe^{3+} (O'Neill et al. 1993). Sample B, containing PV-B, was synthesized in a Re capsule from $Fe_{0.05}Mg_{0.95}SiO_3$ pyroxene with excess SiO_2 and $Fe_{0.1}Pd_{0.9}$ alloy (run H40, 24 GPa, 1900 K, 100 min.). The presence of noble metal alloy in the PV-B run was designed to increase oxygen fugacity in a similar way to runs synthesized in a Re capsule alone (Woodland and O'Neill 1997, for discussion of buffering techniques). The presence of ReO_2 identified in the XRD pattern of PV-B suggests that oxygen fugacities were close to those of the Re-ReO_2 buffer (Pownceby and O'Neill 1994), that is 5 to 6 log-bar units more oxidizing than PV-A under equivalent *P-T* conditions. Electron microprobe analyses (EMPA) of PV-A and PV-B run products gave stoichiometries of $Mg_{0.95}Fe_{0.05}SiO_3$ and $Mg_{0.951}Fe_{0.062}SiO_3$ respectively. EMPA of the metal alloy in PV-B showed loss of Fe and gain of Re. Uncertainties in the Mg and Fe contents from five

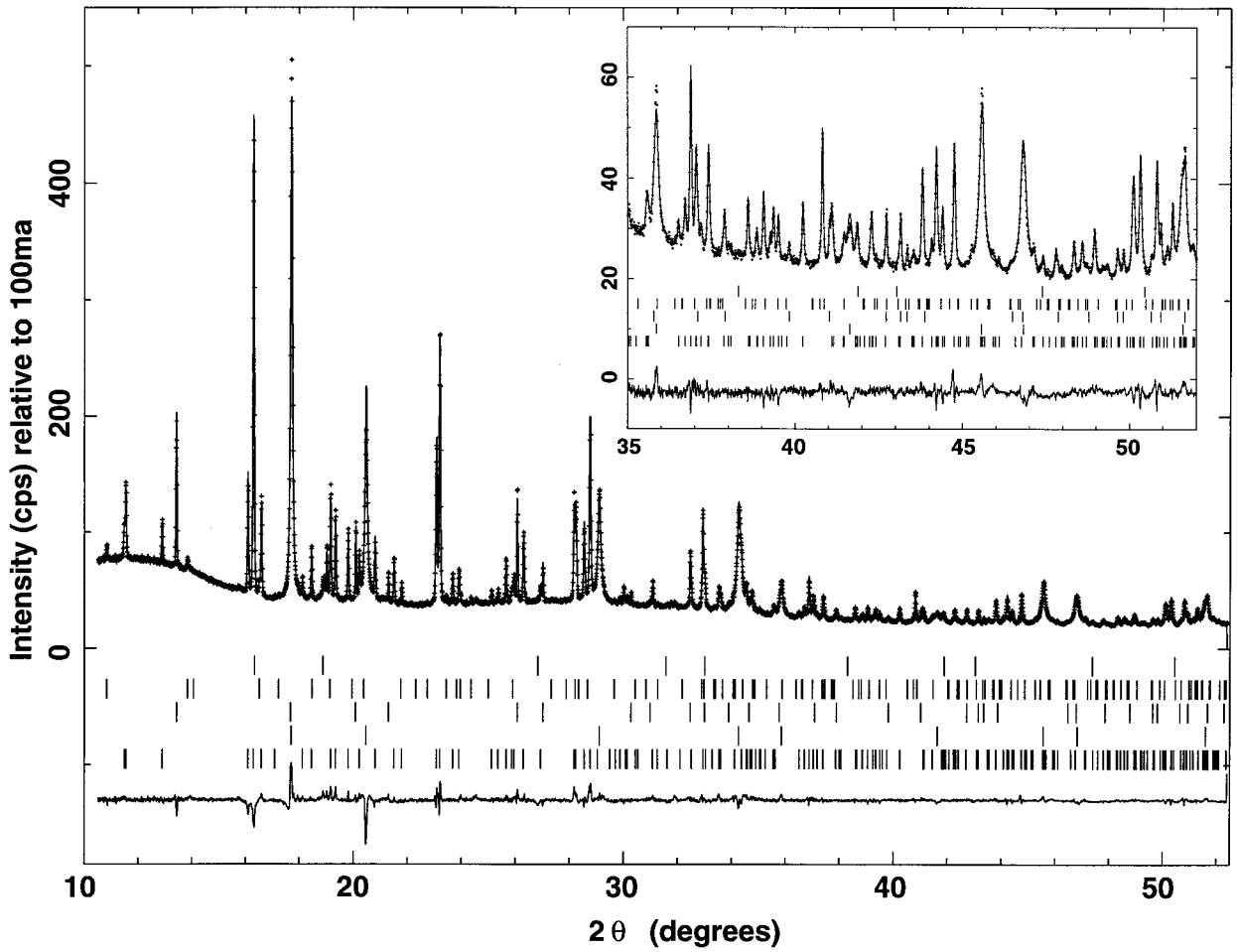

FIGURE 2. Symbols are as in Figure 1. The tick marks below the observed pattern indicate allowed peak positions (from the bottom to the top) of PV-B, the metal alloy, stishovite, ReO_2, and (Mg,Fe)O. Inset is expanded cps scale.

analyses were better than 0.01, but a conservative estimate of 0.02 is more likely as a result of the instability of the perovskite phase under the electron beam.

Mössbauer data were fitted taking into account Fe^{n+} absorption (McCammon 1998) and indicate $Fe^{3+}/\Sigma Fe$ for PV-A was 0.094 ± 0.014 (revised upward from the measurements of McCammon et al. 1992, but assumed to be the minimum Fe^{3+} concentration corresponding to synthesis at minimum f_{O_2}). Recent measurements on compositions with higher Fe^{3+} synthesized in a Re capsule alone (McCammon 1998) indicate that $Fe^{3+}/\Sigma Fe$ is 0.16 ± 0.03 and the hyperfine parameters show double site occupancy for Fe^{3+} (McCammon 1998). The $Fe^{3+}/\Sigma Fe$ for sample PV-B studied here is also close to this value and confirmed from Mössbauer measurements.

XRD measurements were performed at beamline X7A of the Brookhaven National Synchrotron Light Source (NSLS). Data sets for Rietveld refinement were collected with radiation monochromatized and focused in the horizontal plane by an asymmetrically cut Si(220) crystal located at the first axis of the diffractometer and bent to cylindrical curvature. The crystal was designed to provide radiation with a wavelength of ~0.7 Å with $\Delta\lambda/\lambda$ of the order of 3×10^{-4}. The data were collected with a linear position-sensitive detector (PSD) mounted on the 2θ arm 45 cm from the sample, providing optimum tradeoff between resolution and diffracted intensity, as previously described for use with the diamond-anvil cell (Jephcoat et al. 1992). Data were collected in frames with the PSD at overlapping fixed positions, and the data from these frames were then normalized to the incident beam intensity and averaged together to produce a continuous data set. A powder fragment from each multi-anvil run product was mounted in a glass capillary and spun continuously about an axis perpendicular to the incident beam during pattern collection. Fe edge data were obtained with a channel-cut, Si(111) monochromator tuned to ~1.74 Å in place of the asymmetrically cut Si(220) crystal. Wavelengths were calibrated with CeO_2 or silicon powder standards.

Powder data were input directly into the GSAS structure refinement code (Larson and von Dreele 1987) im-

TABLE 1. Cell constants for selected $(Mg,Fe)SiO_3$ perovskite samples

Sample	*a* (Å)	*b* (Å)	*c* (Å)	*V* (Å³)	Reference
PV-A	4.7839(2)	4.9294(2)	6.9000(3)	162.72(2)	This work
PV-B	4.78517(6)	4.93227(7)	6.90484(9)	162.966(5)	This work
$Mg_{0.981}Fe_{0.028}Cr_{0.011}Si_{0.979}O_3$	4.7823(3)	4.9331(3)	6.9026(8)	162.84(2)	Kudoh et al. (1990)
$Mg_{0.95}Fe_{0.05}SiO_3$	4.7817(5)	4.9304(4)	6.9018(4)	162.72(2)	Ito and Yamada (1982)
$Mg_{0.880}Fe_{0.106}Si_{1.007}O_3$	4.7918	4.9312	6.9050	163.16	Parise et al. (1990)

plementing the Rietveld technique (Rietveld 1969). The code allowed refinement of several phases simultaneously, which was an advantage given the presence of impurity materials in the samples. Peak shapes were fit with Voigt functions, and backgrounds were subtracted after linear interpolation.

RESULTS

Analysis of the powder patterns indicate that both samples contained stishovite and (Mg,Fe)O. Sample B also contained excess metal with a composition of $Pd_{0.85}Re_{0.13}Fe_{0.02}$ together with ReO_2.

For Sample A, data to a maximum 2θ value of 42° were collected at 0.69912(4) Å, corresponding to a minimum *d*-spacing of 0.98 Å. The final model included the main orthorhombic *Pbnm* perovskite phase of composition $(Mg_{0.95}Fe_{0.05})SiO_3$ and stishovite (SiO_2). Starting parameters for the atomic coordinates of perovskite and stishovite were taken from previous investigations (Parise et al. 1990; Hyde and Andersson 1989). Given the lower 2θ values collected for this sample and presence of weak reflections that could not be assigned to a known phase, three regions of the pattern (18.06–18.51, 19.52–20.22, and 34.26–35.73°) containing dominant peaks due to Fe and (Mg,Fe)O were excluded from the refinement.

For Sample B, data to a maximum 2θ value of 52.4° were collected at 0.69017(4) Å, corresponding to a minimum *d*-spacing of 0.78 Å. No regions of the pattern were excluded and five phases were refined simultaneously in the model: the main orthorhombic perovskite phase PV-B, stishovite, $Pd_{0.85}Re_{0.13}Fe_{0.02}$, (Mg,Fe)O, and ReO_2. Starting lattice parameters for PV-B, (Mg,Fe)O, and stishovite, were taken from the previous refinement. Lattice parameters of the metal were assumed to start close to those of Pd, and ReO_2 parameters were obtained from Magnéli (1957). Powder-diffraction patterns for PV-A (Fig. 1) and PV-B (Fig. 2) show the observed data, as well as calculated and difference profiles. Unit-cell parameters (corrected for zero-point errors) obtained are in Table 1 together with results from previous studies; positional parameters are in Table 2; selected distances are in Table 3. The final *R*-factors for the refinement of the PV-A data set are: R_p = 10.2%, R_{wp} = 12.7%, R_E = 10.1%, χ^2 = 1.58 and R_F^2 (PV-A) = 15.2%. The final *R*-factors for the refinement of the PV-B data set are: R_p = 2.70%, R_{wp} = 3.79%, R_E = 1.66%, χ^2 = 5.19 and R_F^2 (PV-B) = 5.81%. The higher *R*-factors for PV-A result from poorer counting statistics and smaller data regions included in the refinement compared to PV-B.

Data were collected near to the Fe K-edge (7.112 keV ≡ 1.7433 Å) on both samples to minimize the real anomalous scattering term. The excess heavy metal alloy mixed with PV-B resulted in significant attenuation at the wavelength of the Fe K-edge. Figure 3 shows the data for PV-A collected approximately 6 eV below the Fe K-edge at 1.7448 Å.

DISCUSSION

Both samples predominantly contained the orthorhombic $(Mg,Fe)SiO_3$ perovskite phase, as well as small amounts of stishovite and (Mg,Fe)O. For Sample A, we observed some Fe metal was present, and for the sample containing PV-B both $Pd_{0.85}Re_{0.13}Fe_{0.02}$ alloy and ReO_2 were present. These phases are unreacted starting materials or byproducts formed from the O buffers including the capsule. For sample B, in which five phases were refined and no regions of the pattern were excluded, an excellent fit was obtained (Fig. 2) indicating the applicability of high-resolution data and the Rietveld technique. Based on the relative phase fractions, the sample

TABLE 2. Atomic coordinates for PV-A* and PV-B†

Atom	*x*	*y*	*z*	U_{iso}	Fraction
Mg*	0.5068(17)	0.5557(8)	0.2500	0.0061(14)	0.95
Mg†	0.5113(4)	0.5533(3)	0.2500	0.0088(4)	0.94
Fe*	0.5068(17)	0.5557(8)	0.2500	0.0061(14)	0.05
Fe†	0.5113(4)	0.5533(3)	0.2500	0.0088(4)	0.06
Si*	0.5000	0.0000	0.5000	0.0042(14)	
Si†	0.5000	0.0000	0.5000	0.0048(3)	
O(1)*	0.1032(15)	0.4614(17)	0.2500	0.0040	
O(1)†	0.1030(6)	0.4650(7)	0.2500	0.0040	
O(2)*	0.1933(11)	0.2031(12)	0.5472(8)	0.0043	
O(2)†	0.1937(4)	0.2009(4)	0.5528(3)	0.0043	

* Top.
† Bottom.

TABLE 3. Selected bond distances (Å)

PV-A		PV-B	
Mg(Fe)-O1	1.986(10)	Mg(Fe)-O1	2.002(3)
Mg(Fe)-O1	2.068(9)	Mg(Fe)-O1	2.103(4)
Mg(Fe)-O2	2.093(7) ×2	Mg(Fe)-O2	2.047(2) ×2
Mg(Fe)-O2	2.330(8) ×2	Mg(Fe)-O2	2.306(3) ×2
Mg(Fe)-O2	2.377(7) ×2	Mg(Fe)-O2	2.421(2) ×2
Average	2.207	Average	2.207
Si-O2	1.761(6) ×2	Si-O2	1.780(2) ×2
Si-O1	1.804(2) ×2	Si-O1	1.804(1) ×2
Si-O2	1.806(6) ×2	Si-O2	1.806(2) ×2
Average	1.790	Average	1.797

contained 59.8% $(Mg_{0.94}Fe_{0.06})SiO_3$, 6.3% $Pd_{0.85}Re_{0.13}Fe_{0.02}$ alloy, 30.4% stishovite, 0.1% ReO_2, and 3.4% (Mg,Fe)O. This additional information can only be obtained from such a multi-phase refinement and could be useful in experiments where detailed information is required on the type and amount of by-products formed by the addition of components to control oxygen fugacity.

The model used for the orthorhombic perovskite $(Mg,Fe)SiO_3$ phase in the two samples was based on earlier work by Kudoh et al. (1990) and Parise et al. (1990) where Fe^{2+} was definitively located at the A site. Attempts to refine individual *T* factors for all of the atoms were only partially successful, and in both the values for O1 became negative, probably as a result of uncorrected absorption effects. Due to the irregular shapes and polyphase nature of the samples, absorption corrections were not applied. Instead, *T* factors for the A and B sites were refined, and those of O1 and O2 were fixed at the values reported by Horiuchi et al. (1987) for the parent unsubstituted perovskite.

The data for Sample B was of higher quality, and the sample contained a much higher fraction of Fe^{3+}. Therefore, a variety of models were refined to examine the siting of Fe in more detail: Fe was allowed to occupy both the A and B sites with overall composition constrained by the EMPA and *T* factors fixed as noted above. In a second model, *T* factors were also varied. In a third model, *T* factors were fixed and Fe refined on both sites, but with no EMPA constraint. None of the models gave significantly lower *R* factors despite the increase in the

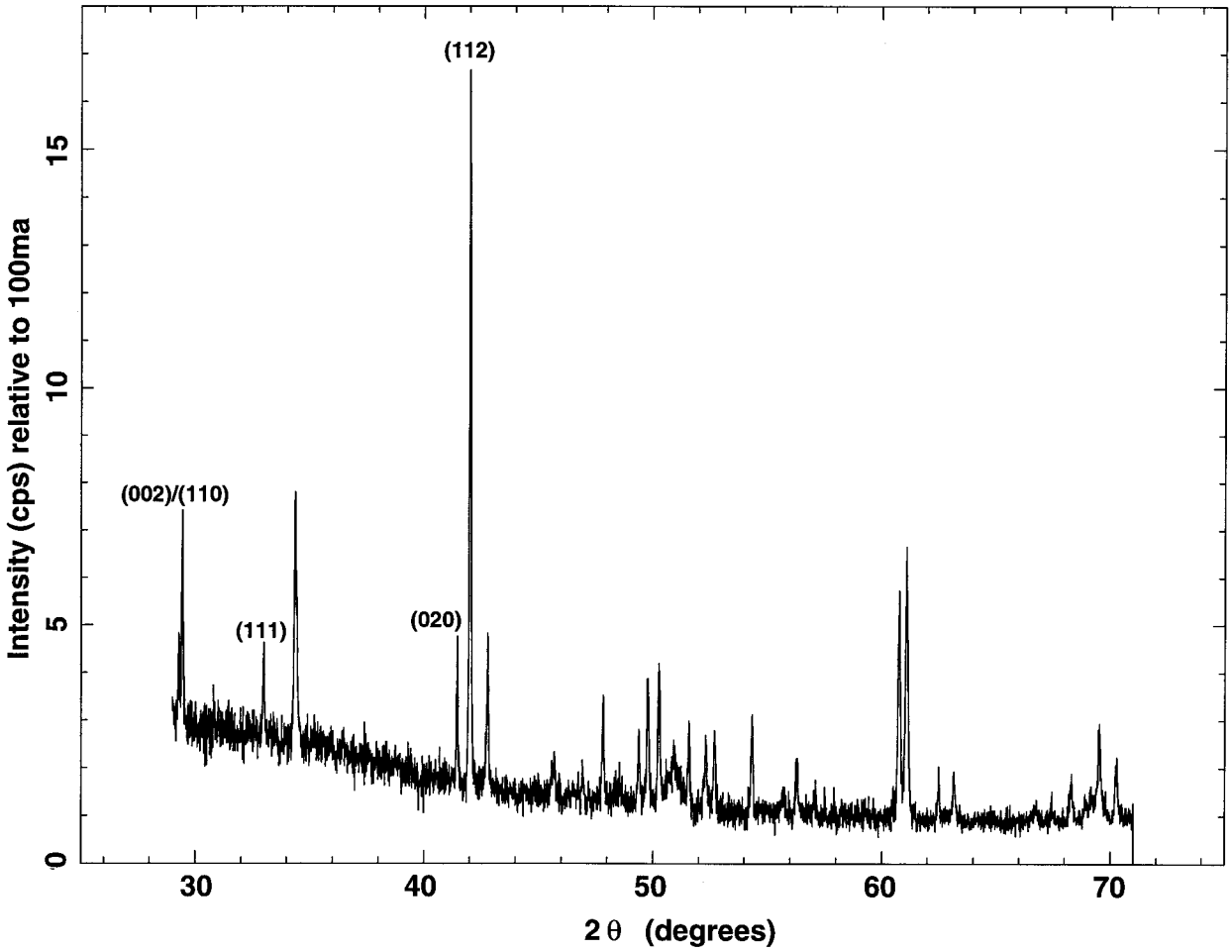

FIGURE 3. Observed diffraction pattern for Sample A collected at 1.7448 Å. Intensities of labeled reflections are calculated and listed in Table 4.

TABLE 4. Intensities for selected reflections from sample A near to the Fe K-edge

hkl	2θ (°)	RI (A site)	RI (B site)	RI (mixed site)	OI
002	29.29	69.3	84.3	76.5	89(13)
110	29.44	179.3	211.9	195.1	228(19)
111	32.98	93.1	88.3	90.7	120(13)
020	41.46	238.1	239.4	238.8	126(25)
112	42.01	1000.0	1000.0	1000.0	1000(32)

Notes: RI = relative intensity; OI = observed intensity; esd's are in parentheses.

number of variables. In all cases, neither the refined site occupancies nor *T* factors provided conclusive evidence that Fe is located on the B site.

Cell parameters for sample PV-B were all significantly greater than for other samples with a similar nominal Fe content (Table 1). The Fe content was calculated as 8 at% based on the refined value of the cell volume and using the regression analysis of Kudoh et al. (1990), which is slightly higher than that derived from EMPA but still within the estimated error. A similar calculation for PV-A gives 4 at%, a value much closer to the average electron microprobe analysis.

Calculated bond distances for both samples (Table 3) compare with previous measurements on samples from other laboratories. Minimal difference appears between the average A-O and B-O distances, even though PV-B has a significantly higher Fe^{3+} content. The A-O and B-O distances may be more regular for PV-B compared to PV-A, but further work is necessary to test for any systematic difference. Significantly higher levels of Fe^{3+} may be necessary before clear evidence for change in structural parameters can be observed by powder X-ray diffraction. The maximum level of Fe^{3+} that can be synthesized in ferromagnesian perovskites has yet to be determined.

In principle, anomalous scattering techniques (Warner et al. 1992) performed at synchrotron sources (where the incident wavelength can be finely tuned) have significant potential for providing independent structural information on the location of the Fe sites and Fe^{2+}/Fe^{3+} distribution. For the data collected at ~6 eV below the Fe K-edge for PV-A (Fig. 3), integrated intensities were calculated using a locally modified version of the program LAZY-PULVERIX (Yvon et al. 1977) with a value of −7 electrons/atom for the Fe *f*' value. This value was estimated using the FPRIME routine within the GSAS package (Larson and von Dreele 1987). Three calculations were performed assuming structures with all of the Fe on the A site, all on the B site and 50% on each site, respectively. The values for five reflections are listed in Table 4, along with those determined from the data. (No absorption correction was applied for this small region of the pattern.) The observed values are of insufficient precision or accuracy to support any of the three models. These preliminary results, however, suggest that the technique could be applied on samples with excess metal removed or at a source optimized for data collection at low energies.

ACKNOWLEDGMENTS

We thank D. Cox for support at Beamline X7A. Research was supported under NATO CRG 890944, the Royal Society, London, and the Natural Environment Research Council grant GR3/7984 (A.P.J.); the National Science Foundation grant EAR-8817263 (L.W.F.); and the Division of Materials Sciences, U.S. Department of Energy, under contract DE-AC02–76CH00016 (J.A.H.). The NSLS is supported by the U.S. Department of Energy, Division of Chemical Sciences and Division of Materials Sciences. M. Kunz and an anonymous reviewer provided useful comments on the manuscript.

REFERENCES CITED

Cox, D.E. (1991) Powder Diffraction. In G.S. Brown and D.E. Moncton, Eds., Handbook on Synchrotron Radiation, Vol. 3, p. 155–200. Elsevier, Amsterdam.

Fei, Y., Virgo, D., Mysen, B.O., Wang, Y., and Mao, H.K. (1994) Temperature-dependent electron delocalization in (Mg,Fe)SiO_3 perovskite. American Mineralogist, 79, 826–837.

Hemley, R.J. and Cohen, R.E. (1992) Silicate perovskite. Annual Review of Earth and Planetary Science, 20, 553–600.

Horiuchi, H., Ito, E., and Weidner, D.J. (1987) Perovskite-type $MgSiO_3$: single crystal X-ray diffraction study. American Mineralogist, 72, 357–360.

Hyde, B.G. and Andersson, S. (1989) Inorganic Crystal Structures. Wiley Interscience, New York.

Ito, E. and Yamada, H. (1982) Stability relations of silicate spinels, ilmenites and perovskites. In S. Akimoto and M.H. Manghani, Eds., High-Pressure Research in Geophysics, p. 405–419. Center for Academic Publications, Tokyo, Japan.

Jephcoat, A.P., Finger, L.W., and Cox, D.E. (1992) High-pressure, high-resolution synchrotron X-ray powder diffraction with a position-sensitive detector. High-Pressure Research, 8, 667–676.

Keppler, H., McCammon, C.A., and Rubie, D.C. (1994) Crystal-field and charge-transfer spectra of (Mg,Fe)SiO_3 perovskite. American Mineralogist, 79, 1215–1218.

Kudoh, Y., Prewitt, C.T., Finger, L.W., Darovskikh, A., and Ito, E. (1990) Effect of Fe on the crystal structure of (Mg,Fe)SiO_3 perovskite. Geophysical Research Letters, 17, 1481–1484.

Larson, A.C. and von Dreele, R.B. (1987) Los Alamos National Laboratory Report No. LA-UR-86–748.

Magnéli, A. (1957) Studies on rhenium oxides. Acta Chemica Scandinavica, 11, 28–33.

McCammon, C.A. (1998) The crystal chemistry of ferric Fe in $Fe_{0.05}Mg_{0.95}SiO_3$ perovskite as determined by Mössbauer spectroscopy in the temperature range 80–293 K. Physics and Chemistry of Minerals, 25, 292–300.

McCammon, C.A., Rubie, D.C., Ross, C.R., Seifert, F., and O'Neill H.St.C. (1992) Mössbauer spectra of $^{57}Fe_{0.05}Mg_{0.95}SiO_3$ perovskite at 80 K and 298 K. American Mineralogist, 77, 894–897.

O'Neill, H.St.C., McCammon, C.A., Canil, D., Rubie, D.C., Ross, C.R., and Seifert, F. (1993) Mössbauer spectroscopy of mantle transition-zone phases and determination of minimum Fe^{3+} content. American Mineralogist, 78, 456–460.

Parise, J.B., Wang, Y., Yeganeh-Haeri, A., Cox, D.E., and Fei, Y. (1990) Crystal structure and thermal expansion of (Mg,Fe)SiO_3 perovskite. Geophysical Research Letters, 17, 2089–2092.

Poirier, J.P., Goddat, A., and Peyronneau, J. (1996) Ferric Fe dependence of the electrical conductivity of the Earth's lower mantle material. Philosophical Transactions of the Royal Society of London, Series A, 354, 1361–1369.

Pownceby, M.I. and O'Neill, H.St.C. (1994) Thermodynamic data from redox reactions at high temperatures. IV. Calibration of the Re-ReO_2 oxygen buffer from EMF and NiO + Ni-Pd redox sensor measurements. Contributions to Mineralogy and Petrology, 118, 130–137.

Rietveld, H.M. (1969) A profile refinement method for nuclear and magnetic structures. Journal of Applied Crystallography, 2, 65–71.

Shen, G., Fei, Y., Hålenius, U., and Wang, Y. (1994) Optical absorp-

tion spectra of $(Mg,Fe)SiO_3$ silicate perovskites. Physics and Chemistry of Minerals, 20, 478–482.

Warner, J.K., Cheetham, A.K., Cox, D.E., and von Dreele, R.B. (1992) Valence contrast between Fe sites in α–Fe_2PO_5: a comparative study by magnetic neutron and resonant X-ray powder diffraction. Journal of the American Chemical Society, 114, 6074–6080.

Wood, B.J. and Nell, J. (1991) High-temperature electrical conductivity of the lower-mantle phase (Mg,Fe)O. Nature, 351, 309–311.

Woodland, A.B. and O'Neill, H.St.C. (1997) Thermodynamic data for Fe-bearing phases obtained using noble metal alloys as redox sensors. Geochimica et Cosmochimica Acta, 61, 4359–4366.

Yvon, K., Jeitschko, and Parthe, E. (1977) LAZY-PULVERIX. Journal of Applied Crystallography, 10, 73–74.

Manuscript received July 7, 1998
Manuscript accepted September 25, 1998
Paper handled by John Parise